PERGAMON

Chaos, Solitons and Fractals 15 (2003) 417–424

CHAOS
SOLITONS & FRACTALS

www.elsevier.com/locate/chaos

Boundary crises, fractal basin boundaries, and electric power collapses

Sura H.C. Marcos, Sérgio R. Lopes, Ricardo L. Viana *

Departamento de Física, Universidade Federal do Paraná, Caixa Postal 19081, 81531-990, Curitiba, Paraná, Brazil

Accepted 29 April 2002

Abstract

Electric power systems are frequently nonlinear and, when faced with increasing power demands, may behave in unpredictable and rather irregular ways. We investigated the nonlinear dynamics of a single machine infinite bus power system model in order to study the appearance of coexistent periodic and chaotic attractors, characterizing multi-stable behavior. The corresponding basins of attraction present fractal boundaries, for which we have determined the uncertain fraction scaling in phase space. The bifurcation diagrams are studied with respect to variations of the mechanical power input and may lead to voltage collapse under certain circumstances, which we relate to a boundary crisis suffered by a chaotic attractor.

Voltage collapse in electric power systems have caused blackouts around the world, with losses of billions of dollars and many side effects as damages in household appliances, increase of crime rates, and car crashes, just to name a few [1]. Although the exact mechanism of a voltage collapse is still a matter of investigation, it is known that in such events the voltage magnitudes at electric power systems decrease rapidly under a heavy load [2]. From a more fundamental point of view, the ubiquitous presence of bifurcations in the dynamic behavior of nonlinear electric power systems may be related to the occurrence of voltage collapses [3]. In this picture, a normal operation of the power system would correspond to a stable equilibrium state. When the production or transmission of electric energy is insufficient to supply an increasing power demand, an electric power system may lose its operational stability through a bifurcation, where the actual state becomes unstable and new stable states are created [4].

The current literature on this subject assigns as possible causes of voltage collapse: (i) a saddle node bifurcation [5], where stable and unstable equilibria coalesce at the bifurcation point and disappear; (ii) a chaotic blue-sky bifurcation [6], where a chaotic attractor collides with an unstable equilibrium, also known as an interior crisis [7,8]. This chaotic attractor is achieved through a flip bifurcation cascade that begins with a limit cycle produced through a supercritical Hopf bifurcation, after which the former stable equilibrium becomes unstable. The connection between these description lies in the fact that the unstable equilibrium that collides with the chaotic attractor coalesces with the stable equilibrium that undergoes a Hopf bifurcation, through a saddle-node bifurcation [9].

Besides voltage collapse, the existence of long-lived chaotic transients is also an issue of major safety concern in the operation of an electric power system. The latter commonly has protective relay devices, designed not to interfere with the transient voltage oscillations. Hence they do not play a stabilizing role, which could be actually necessary to avoid undesirable voltage transients, which may cause severe damage to expensive equipment such as rotor shafts, if the

* Corresponding author. Tel.: +55-44-366-2323; fax: +55-41-267236.
E-mail address: viana@fisica.ufpr.br (R.L. Viana).

0960-0779/03/$ - see front matter © 2002 Published by Elsevier Science Ltd.
PII: S0960-0779(02)00108-X

transient duration is too large. Consequently the occurrence of chaotic transients should be, if not completely avoided, at least diminished to admissible levels.

The link between these two situations is the presence of crises, or abrupt changes in a chaotic attractor due either to its collision with an unstable periodic orbit or with a basin boundary. After a crisis has occurred, the former chaotic attractor either increases its size or disappears, remaining in its place a chaotic transient which eventually decays to some attractor, bounded or at infinity. Thus a voltage collapse may be triggered by a chaotic transient, which drives the electric power system to some asymptotic state out of its normal operational limits. It is thus of paramount importance to characterize and, if possible, to control the causes of voltage collapse related to crises.

From an historical point of view, it has been long recognized the existence of complicated dynamical behavior in electric power systems such as the swing equations [10], single machine quasi-infinite bus-bar system [11], three-machine power networks with exciters [12], five-bus systems [13], and single machine infinite bus (SMIB) model [2], just to cite a representative sample of works on this subject. In this work we focus on the classical SMIB power system of Ref. [14], consisting on an SMIB with a wind-up-type hard limit which is introduced to constrain the control gains in the system voltage. It should be emphasized that while such an SMIB model can be of limited validity for studies of networks with a large number of generators, the dynamics of an SMIB provides valuable insights into what could be expected from the interaction between a single generator and the rest of the power system.

In previous works [12,14] it was found, for an SMIB model, quasi-periodic dynamics in addition to chaotic motion, the latter being studied as an alternative operating condition for a power system, even when there exists an accessible stable equilibrium for the same set of parameter values. In this note we shall focus on some dynamic features of the SMIB model of Ref. [14] which have not hitherto been analyzed in depth, namely the existence of boundary crises, multi-stability, and the corresponding basin boundary structure. Complex systems such an SMIB typically exhibit more than one possible attractor to which its trajectories in phase space asymptote, depending on the basin where the initial condition is placed. These attractors can be either periodic, quasi-periodic, or chaotic, not to mention the case of an (unbounded) attractor at infinity, related to the chaotic transients we argue to be related to a voltage collapse.

On the other hand, low-period stable attractors are related to operational regimes for electric power systems, and most engineering systems in general [9]. Multi-stability implies the coexistence of many possible operational regimes, from which we could in principle choose the one that gives us a better performance. Hence, we need to understand the basin boundary structure of the system, which may be rather involved since the boundaries are often a mixture of smooth and fractal curves. In the latter case, the fraction of uncertain initial conditions in the phase space scales in a power-law fashion with the size of the admissible error in determining the initial condition. This leads to final-state sensitivity, i.e., in order to decrease the uncertain fraction by a given amount, no matter how small, we would have to improve substantially the accuracy in determining the initial condition.

The theoretical model of Ref. [14] aims to describe the interaction of a single generator with a large electric power system, the latter being represented by an equivalent SMIB system, connected to the generator (a synchronous machine coupled to a turbine) by a transmission line (Fig. 1). The generator is dynamically characterized by the machine angle $\delta(t)$, the frequency deviation $\omega(t)$, and the internal flux decay $E'(t)$ representing the voltage magnitude behind the transient reactance. There is a fourth dynamical variable, $E_{\mathrm{fd}}(t)$, which represents the field excitation voltage.

The machine angle dynamics is described by the so-called swing equations [15]

$$\frac{\mathrm{d}\delta}{\mathrm{d}t} = 2\pi f_0(\omega - 1), \tag{1}$$

$$\frac{\mathrm{d}\omega}{\mathrm{d}t} = -\frac{D}{2H}(\omega - 1) + \frac{1}{2H}(P_{\mathrm{T}} - P_{\mathrm{G}}), \tag{2}$$

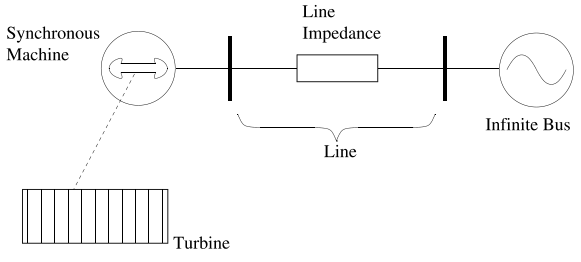

Fig. 1. Schematic view of a SMIB power system.

where $M \equiv 2H$ is the moment of inertia, f_0 is a constant linear frequency, D is the damping factor, P_T is the mechanical power input, and P_G is the electrical power generated.

On the other hand, the time behavior of the voltage magnitude is governed, for SMIB systems, by the following single axis flux decay equation [12,14]

$$\frac{dE'}{dt} = \frac{1}{T'_{d0}}\left[-\left(\frac{x_d + x}{x'_d + x}\right)E' + \left(\frac{x_d - x'_d}{x'_d + x}\right)\cos\delta + E_{fd}\right], \tag{3}$$

where T'_{d0} is the direct axis transient time constant, x_d is the synchronous reactance, x'_d is the transient reactance, and x is the transmission line parameter.

The role of the wind-up-type hard limits is to set the control gains of the excitation voltage. The presence of such excitation field control in the generator machine can be represented by a single time-constant transfer function. We will use, according to Ref. [14], a piecewise linear model which still retains, in spite of its simplicity, some general features present in realistic transfer functions of turbogenerator units. The output of the wind-up limiter, E_{fd}, for a piecewise linear model, is

$$E_{fd} = \begin{cases} E_{fd_{max}} & \text{if } V_R > E_{fd_{max}}, \\ V_R & \text{if } E_{fd_{min}} \leqslant V_R \leqslant E_{fd_{max}}, \\ E_{fd_{min}} & \text{if } V_R < E_{fd_{min}}, \end{cases} \tag{4}$$

where V_R is the input signal in the wind-up hard limit, which constrains the output E_{fd} to lie in an interval whose endpoints are $E_{fd_{min}}$ and $E_{fd_{max}}$.

With the hard-limit control adopted, the equation governing the time evolution of the control input signal V_R is

$$\frac{dV_R}{dt} = \frac{1}{T_A}[-K_A(V_R - V_{ref}) - V_R], \tag{5}$$

where T_A is the excitation control time constant, K_A is the control gain, V_{ref} is the reference bus voltage, and V is the bus voltage at the generator bus terminal for the SMIB representation, given by

$$V = \sqrt{\left(\frac{xE' + x'_d\cos\delta}{x + x'_d}\right)^2 + \left(\frac{x_q\sin\delta}{x + x_q}\right)^2}, \tag{6}$$

in which x_q is a system reactance. In order to close the system of algebraic and differential equations of the SMIB model here studied, we also need a relation for the generated power

$$P_G = \frac{E'\sin\delta}{x + x'_d} + \frac{(x'_d - x_q)\sin 2\delta}{2(x + x_q)(x + x'_d)}. \tag{7}$$

The phase space for the power system of an SMIB is thus four-dimensional, in that a given state is characterized by values of the dynamical variables $\delta(t)$, $\omega(t)$, $E'(t)$, and $V_R(t)$. By neglecting saturation effects, during the system operation the synchronous machine parameters M, x_d, x'_d, and T'_{d0} can be considered constants, as well as the transmission line parameter x, the mechanical power input P_T, the voltage set-point V_{ref}, the gain K_A, and the damping D. The values for these parameters which are to be used throughout this paper were taken from Refs. [12,14].

The four-dimensional vector field governing the dynamics of the SMIB model is given by Eqs. (1)–(5), and has to be supplemented by the algebraic equations (6) and (7), as well as the control law (4). Since we are investigating the effect of a wind-up hard limiter in an SMIB system, it turns out that an interesting variable to focus our attention is the input signal voltage $V_R(t)$. Moreover, we choose P_T, the mechanical power input, as the tunable parameter with respect to which the dynamical response of the system is considered. The numerical computations in this paper were done by using a 12th order Adams method, from the LSODA package [16].

The linearized dynamics of the SMIB model has been investigated by Ji and Venkatasubramanian [14], who determined its equilibrium points and studied their local stability, as well as the occurrence of Hopf and saddle-node bifurcations. By varying also the damping parameter D, a period-doubling cascade has also been observed leading to chaos. In particular, a funnel strange attractor in the (E', δ, ω) phase space has been thoroughly analyzed. In a later paper [12] there has been reported the occurrence of multi-stable behavior, or the coexistence of four different attractors—a stable equilibrium, a stable limit cycle and two chaotic attractors. In this work we will study the basin boundary structure related to this multi-stable scenario, as well as some of the changes on the attractors in virtue of crises.

The dependence of the coexisting periodic and chaotic attractors on the control parameter P_T is illustrated by the bifurcation diagrams depicted in Fig. 2, where we plot the input voltage V_R for fixed values of the other dynamical

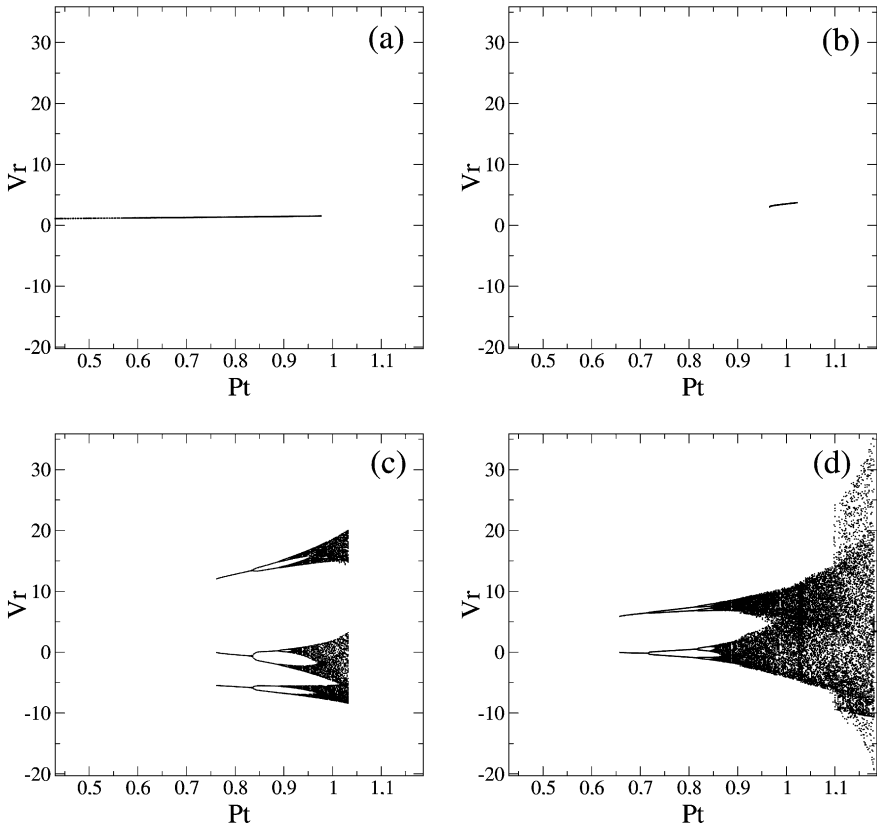

Fig. 2. Bifurcation diagram for the input voltage V_R versus the mechanical power input P_T. Parameters were taken from Refs. [12,14].

variables. There are four coexisting attractors, each of them being represented separately. For small values of P_T only a stable equilibrium near zero is observed (Fig. 2a), corresponding to a desirable performance of the power system. This fixed point loses stability at $P_{TH} \approx 0.9775$, where a sub-critical Hopf bifurcation occurs. A cyclic fold bifurcation at $P_T \approx 0.966$ creates a stable limit cycle which disappears at $P_T \approx 1.027$ through a reverse cyclic fold bifurcation [12] (Fig. 2b).

As the mechanical power is increased, we observe that at $P_T = P_{T_{SN}} \approx 0.655$ a period-2 orbit is born through a saddle-node bifurcation, of which only the stable branch is plotted in Fig. 2d. This period-2 orbit leads to chaos through a period-doubling cascade after $P_{T\infty} \approx 0.85$, initially with two band which merge at $P_T \approx 0.96$ into a single chaotic band, which suddenly increases its size slightly after $P_T = 1.1$. Basically the same mechanism is responsible for the creation of a period-3 orbit at 0.75 which undergoes a period-doubling cascade to a chaotic region (Fig. 2c). This chaotic region ends up suddenly at $P_{T_{CR}} \approx 1.04$ through an interior crisis, which results from the collision of the single chaotic band with the unstable period-3 branch not plotted in the diagram [7]. These results show the existence of multi-stable behavior in a representative portion of the interval of the values allowed for the power input parameter. Each coexistent attractor has its own basin of attraction, with a typically involved structure in the phase space, characterized by fractal boundaries [17]. If we consider the ubiquitous presence of noise in complex systems [18], it may well happen that a trajectory visiting the neighborhood of some complicated basin boundary receives noise-induced kicks that make it jump to another basin. Hence, from the point of view of an engineering system, the existence of multiple attractors may be as harmful as chaos, roughly speaking, because the noise-induced attractor hopping may cause high-amplitude jumps with a nonzero probability [19]. It is important to know first the basin boundary structure related to each coexisting attractor in order to gather information about the possibilities of attractor hopping due to external noise and its practical consequences.

Since the phase space is four-dimensional, we choose to work with a projection of it along a two-dimensional subspace like (δ, E'), the other dynamical variables being held constant: $\omega = 1.0$ and $V_R = 3.5$. We consider the basin boundary structure in the (δ, E') projection of the full phase space, for cases exhibiting multi-stable behavior. Fig. 3 was obtained for $P_T = 1.027$, where we have coexistence of four different attractors, represented by different shades of gray:

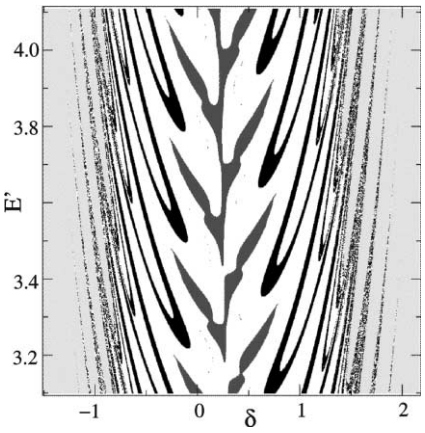

Fig. 3. A projection of the phase space, for $P_T = 0.97$, $\omega = 1.0$, and $V_R = 3.5$, showing the basins of coexistent attractors: limit cycle (dark gray); infinity (light gray), and chaotic attractors from cascades of a period-2 (white) and period-3 (black) orbits.

the limit cycle (dark gray); the chaotic attractors arising from period-doublings of period-2 (white) and period-3 (black) orbits; and also an unbounded attractor at infinity (light gray). Note that, for this value of P_T, the fixed point (which basin was formerly contained in the dark gray region) has already lost stability, and the initial conditions belonging to its basin will now asymptote to the limit cycle.

The fishbone aspect of Fig. 3 suggests a highly complex structure, particularly for the boundary between the basins of the two chaotic attractors (the black and white regions). Magnifications (Figs. 4 and 5) of small boxes picked up from a region containing this boundary suggest the occurrence of fractal basin boundaries, since the basins have transversally a structure akin to a Cantor set. It has been long recognized that in this case one has *final state sensitivity*. Any initial condition in the phase space is determined up to a given uncertainty ϵ, which in general can be represented as a ball centered at the phase point with radius ϵ. If this error ball intersects the basin boundary between two asymptotic states of the system, one is unable in principle to determine to which attractor the system will approach. In this case the initial condition is said to be ϵ-*uncertain* [20]. Now we repeat this process for a large number of randomly chosen points in the phase space, according to the natural measure of the attractor, and compute the ratio $f(\epsilon)$, the *uncertain fraction*, between the number of ϵ-uncertain initial conditions to the total number of points chosen (Fig. 7).

When the basin boundary is a smooth curve, the uncertain fraction scales linearly $f(\epsilon) \sim \epsilon$. On the other hand, if the boundary has a fractal nature we expect a power-law scaling: $f(\epsilon) \sim \epsilon^{\alpha}$, where α is the *uncertainty exponent* [21], or the rate at which we have to increase the accuracy in determining the initial condition, in order to reduce the uncertain fraction $f(\epsilon)$ by a given amount. The uncertainty exponent α is related to the basin boundary box-counting dimension d by $\alpha = D - d$, where $D = 4$ is the phase-space dimension [20]. We apply this numerical procedure to evaluate the dimension of the basin boundary between black and white basins in Fig. 3. In Fig. 6 we plot the corresponding uncertain

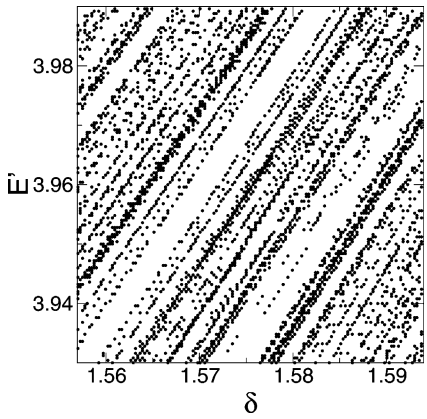

Fig. 4. Magnification of a small box of the previous figure.

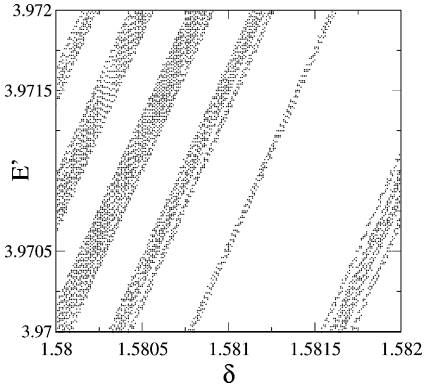

Fig. 5. Same as previous, with a finer scale.

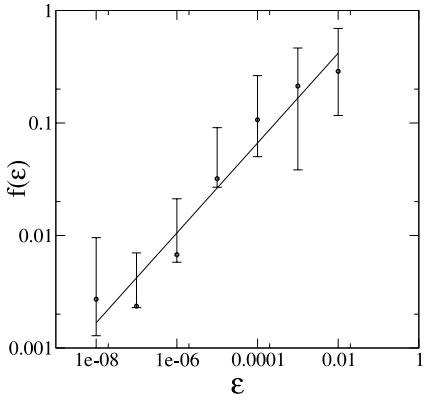

Fig. 6. Uncertain fraction of phase space projection as a function of the radius of error balls centered at points randomly chosen within the box shown in Fig. 3.

fraction versus the size of the error balls ϵ, with a least-squares fit as a power-law scaling, with a slope $\tilde{\alpha} = 0.400 \pm 0.041$. Since $\tilde{\alpha} < 1$ it turns out that a specified decrease in the uncertainty of initial conditions yields only a relatively small reduction of the uncertainty about to which attractor the resulting trajectory will asymptote. The estimated basin boundary dimension is thus $d \approx 3.6$.

The bifurcation diagram of Fig. 2 indicates the sudden disappearance of the chaotic attractor for a critical perturbation $P_{\mathrm{T_{CR}}} = 1.17477$, after which almost all trajectories asymptote to infinity. This is an example of a boundary crisis, in which the chaotic attractor collides at $P_{\mathrm{T_{CR}}}$ with its own basin boundary and disappear in an abrupt way, giving place to a non-attracting set with a dense orbit (a chaotic saddle) [8]. Let the bifurcation parameter be not far from the critical value $P_{\mathrm{T_{CR}}}$. A trajectory evolving from an initial condition placed near the chaotic saddle will wander in an irregular way through the remnant of the attractor, generating a typically long chaotic transient, which eventually decays to infinity, in this specific case. We denote by τ the duration of the chaotic transient generated by a single initial condition near the remnant of that chaotic attractor existing for $P_{\mathrm{T}} < P_{\mathrm{T_{CR}}}$.

Due to the highly involved boundary structure of the basin of infinity, it is expected that the duration of the chaotic transient be strongly dependent on where we pick up the initial condition. A chaotic saddle is comprised by an infinite number of intersecting stable and unstable manifolds [8]. A point placed exactly on some of these manifolds would generate a trajectory staying on the manifold for all times, and never escapes to infinity. There results that, if an initial condition is chosen very close to some of these manifolds it will stay longer in the attractor remnant, compared to initial conditions farther from the saddle, resulting in larger transient times. We can cope with this diversity by considering a large number of randomly chosen initial conditions in some region containing the interesting part of the basin boundary structure, and numerically computing the transient time τ for each of them, with average $\langle\tau\rangle$. The transient times are expected to follow a Poisson distribution

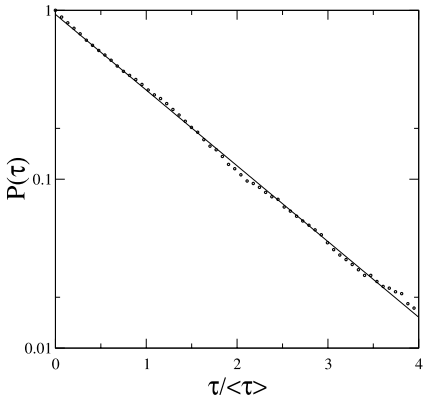

Fig. 7. Fraction of orbits that do not asymptote to infinity after time τ, for $P_T = 1.1758577$.

$$P(\tau) = \frac{1}{\langle\tau\rangle} \exp\left(-\frac{\tau}{\langle\tau\rangle}\right). \tag{8}$$

There are strong theoretical arguments supporting this statistics [22], but it is possible to justify its use through a heuristic argument. When considering the post-critical dynamics there are just two possible outcomes for a trajectory from an initial condition near the chaotic saddle: it will either escape or remain in the immediate vicinity of the chaotic saddle for a long time. However, since the saddle has zero Lebesgue measure in phase space, the probability of escape is much larger than of not doing so. From the statistical point of view the problem would be cast into a binomial probability distribution, but since the probability of one event is very small compared to the other one, it will reduce to a Poissonian one. We have numerically verified this fact by plotting in Fig. 7 the fraction of orbits that do not escape after a time τ, normalized according to its mean $\langle\tau\rangle = 88144.56$, for a given value of $P_T > P_{T_{CR}}$. For a large number of initial conditions, randomly scattered over a limited region of the projected phase space ($1.568 < \delta < 1.588$ and $3.256 < E' < 3.580$) we found a least-squares fitted curve in agreement with Eq. (8), which predicts a slope equal to unity.

As we approach from above the crisis threshold at $P_{T_{CR}} = 1.17477$ the average duration of the chaotic transient $\langle\tau\rangle$ is expected to increase in a power-law fashion [8]

$$\langle\tau\rangle \approx K(P_T - P_{T_{CR}})^{\gamma}, \tag{9}$$

where the characteristic exponent γ is negative, and is related to the eigenvalues of the unstable periodic orbit involved in the collision between the attractor and its basin boundary at $P_{T_{CR}}$ [8]. In Fig. 8 we plot the average transient time

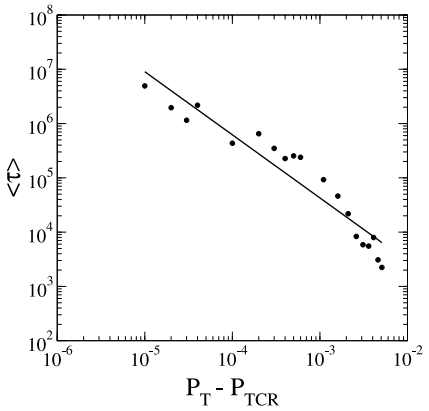

Fig. 8. Average transient time versus the difference $P_T - P_{T_{CR}}$. The fitted line corresponds to coefficients $K = 13.876$ and $\gamma \approx 1.163$ in Eq. (9).

versus the difference $P_T - P_{T_{CR}}$ for a number of chaotic transients arising from randomly chosen initial conditions. The least-squares fit to the numerical data confirms the scaling (9) with an exponent $\gamma = -1.163 \pm 0.088$.

In conclusion, we have analyzed a theoretical model of a power system consisting on a SMIB with a wind-up-type hard limit, with four dynamical variables. Due to weak dissipation there is multi-stable behavior, characterized by a coexistence of periodic and chaotic attractors, with a complicated basin structure. We found that the basin boundaries are typically of a fractal nature. Using the uncertainty dimension technique we found a dimension close to that of the phase space itself, indicating that the basin boundary occupies most of the available space, what is a clear indication of the complexity inherent to the basin structure. Another issue considered was the boundary crisis occurring for a critical value of the mechanical power, for which we have found a power-law scaling for the average duration of the chaotic transient.

Acknowledgements

This work was made possible by partial financial support from the following Brazilian government agencies: CNPq, Fundação Araucária (State of Paraná), and FUNPAR (UFPR). One of us (RLV) would like to thank Professor Celso Grebogi (USP) for useful suggestions.

References

[1] Dobson I, Glavitsch H, Liu C-C, Tamura Y, Vu K. Voltage collapse in power systems. Circuits Dev 1992:40–5.
[2] Ohta H, Ueda Y. Unstable limit cycles in an electric power system and basin boundary of voltage collapse. Chaos, Solitons Fractals 2001;12:159–72.
[3] Chiang HD, Liu CW, Varaiya PP, Wu FF, Lauby MG. Chaos in a simple power system. IEEE Trans Power Systems 1993;8:1407–17.
[4] Rosehart WD, Canizares CA. Bifurcation analysis of various power system models. Electrical Power Energy Systems 1999;21:171–82.
[5] Dobson I, Chiang HD. Towards a theory of voltage collapse in electric power systems. Systems Control Lett 1989;13:253–62.
[6] Wang HO, Abed EH, Hamdan AMA. Bifurcations, chaos, and crises in voltage collapse of a model power system. IEEE Trans Circuits Systems I 1994;41:294–302.
[7] Grebogi C, Ott E, Yorke JA. Chaotic attractors in crisis. Phys Rev Lett 1982;48:1507–10.
[8] Grebogi C, Ott E, Yorke JA. Crises, sudden changes in chaotic attractors, and transient chaos. Phys D 1983;7:181–200.
[9] Kapitaniak T. Chaos for engineers. New York, Berlin, Heidelberg: Springer; 2000.
[10] Kopell N, Washburn RB. Chaotic motion in the two-degree-of-freedom swing equations. IEEE Trans Circuits Systems I 1982;29:738–46.
[11] Nayfeh MA, Hamdan AMA, Nayfeh AH. Chaos and instability in a power system—primary resonance case. Nonlinear Dyn 1990;1:313–39.
[12] Ji W, Venkatasubramanian V. Coexistence of four different attractors in a fundamental power system model. IEEE Trans Circuits Systems I 1999;46:405–9.
[13] Dobson I, Lu L. New methods for computing a closest saddle node bifurcation and worst case load power margin for voltage collapse. IEEE Trans Power Systems 1993;8:905–13.
[14] Ji W, Venkatasubramanian V. Hard-limit induced chaos in a fundamental power system model. Electrical Power Energy Systems 1996;18:279–95.
[15] Vittal V, Bergen AR. Power systems analysis. New York: Prentice Hall; 1999.
[16] Hindmarch AC. ODEPACK: a systematized collection of ODE solvers. In: Stepleman RS et al., editors. Scientific Computing. Amsterdam: North-Holland; 1983. p. 55;
Petzold LR. SIAM J Sci Stat Comput 1983;4:136.
[17] Feudel U, Grebogi C. Multistability and the control of complexity. Chaos 1997;7:597–604.
[18] Kapitaniak T. Chaos in systems with noise. Singapore: World Scientific; 1990.
[19] Kraut S, Feudel U, Grebogi C. Preference of attractors in noisy multistable systems. Phys Rev E 1999;59:5253–60.
[20] McDonald SW, Grebogi C, Ott E. Fractal basin boundaries. Phys D 1985;17:125–53.
[21] McDonald SW, Grebogi C, Ott E. Final state sensitivity: an obstruction to predictability. Phys Lett A 1983;99:415–8.
[22] Ott E. Chaos in dynamical systems. Cambridge: Cambridge University Press; 1993.